Journal of Materials Science and Chemical Engineering, 2024, 12, 84-103
https://www.scirp.org/journal/msce
ISSN Online: 2327-6053
ISSN Print: 2327-6045

Hexavalent Chromium Cr (VI) Removal from Water by Mango Kernel Powder

Amadou Sarr Gning[1], Cheikh Gaye[1], Antoine Blaise Kama[2], Pape Abdoulaye Diaw[3,4*], Diène Diégane Thiare[4], Modou Fall[1]

[1]Laboratoire de Chimie Physique Organique et d'Analyses Environnementales (LCPOAE), Université Cheikh Anta Diop, Dakar, Sénégal
[2]Equipe Chimie des Matériaux Inorganique et Organique (ECMIO), Université Alioune Diop, Bambey, Sénégal
[3]Equipe des Matériaux, Electrochimie et Photochimie Analytiques (EMEPA), Université Alioune Diop, Bambey, Sénégal
[4]Laboratoire de Photochimie et d'Analyse (LPA), Université Cheikh Anta Diop, Dakar, Sénégal
Email: *papeabdoulaye.diaw@uadb.edu.sn

How to cite this paper: Gning, A.S., Gaye, C., Kama, A.B., Diaw, P.A., Thiare, D.D. and Fall, M. (2024) Hexavalent Chromium Cr (VI) Removal from Water by Mango Kernel Powder. *Journal of Materials Science and Chemical Engineering*, **12**, 84-103.
https://doi.org/10.4236/msce.2024.121007

Received: November 22, 2023
Accepted: January 28, 2024
Published: January 31, 2024

Abstract

Metal trace elements (MTE) are among the most harmful micropollutants of natural waters. Eliminating them helps improve the quality and safety of drinking water and protect human health. In this work, we used mango kernel powder (MKP) as bioadsorbent material for removal of Cr (VI) from water. Uv-visible spectroscopy was used to monitor and quantify Cr (VI) during processing using the Beer-Lambert formula. Some parameters such as pH, mango powder, mass and contact time were optimized to determine adsorption capacity and chromium removal rate. Adsorption kinetics, equilibrium, isotherms and thermodynamic parameters such as ΔG°, ΔH°, and ΔS°, as well as FTIR were studied to better understand the Cr (VI) removal process by MKP. The adsorption capacity reached 94.87 mg/g, for an optimal contact time of 30 min at 298 K. The obtained results are in accordance with a pseudo-second order Freundlich adsorption isotherm model. Finally FTIR was used to monitor the evolution of absorption bands, while *Scanning Electron Microscopy* (*SEM*) and Energy Dispersive X-ray Spectroscopy (EDS) were used to evaluate surface properties and morphology of the adsorbent.

Keywords

Adsorption, Chromium, Mango Kernel Powder, Spectroscopy Analysis, Water Treatment

1. Introduction

Nowadays, water pollution by Metal Trace Elements (MTE) is of growing con-

cern as it represents a major risk to human and environmental health due to their toxicity and their non-biodegradability [1] [2]. Among the MTE, hexavalent and trivalent chromium are the two most stable and widespread oxidation states of chromium in the environment. Chromium (Cr) is one of the most abundant MTE on earth [3] [4]. It can be directly or indirectly induced by humans through various activities. The modernization of cities through sanitation (sewage, plumbing, etc.) and industrialization (electroplating, tanning, cooling of industrial waters, oil refining, textile dying, wood preservatives, etc.) have led to the massive presence of chromium in ecosystems [5]. Quarrying activities (chromite ores, sedimentary rocks, igneous rocks, etc.) can also be sources of contamination of natural waters [6]. Chromium is rarely found in the earth's crust as a metal but as ionic compounds in the aquatic environment. Cr (VI) species have higher solubility and mobility in aqueous media and is considered as the most harmful form. It is mutagenic, carcinogenic, teratogenic and 500 times more toxic than Cr (III) [7] [8]. In low doses, trivalent chromium is an important micronutrient in human metabolism through its participation in carbohydrate and lipid synthesis [9]. Cr (III) is involved in the maintenance of glucose, cholesterol and triglyceride levels [10]. Insufficient levels of trivalent chromium in the body result in a decrease in insulin secretion [11]. Cr (VI) is one of the most toxic pollutants with harmful properties for the human body, due to its ability to cross biological membranes and its high oxidizing properties [12] [13]. Contamination with Cr (VI) causes nausea, diarrhea, poor liver and kidney function, skin problems, respiratory problems and internal bleeding [10]. The limit levels of chromium and its derivatives are 1 μg/L for Cr (VI) and 8 μg/L for Cr (III) in freshwater, 8 μg/L for Cr (VI) and 5 μg/L for Cr (III) in irrigation water [14]. According to international standards, the limit concentration of hexavalent chromium in drinking water is 0.05 mg/L and the standard for industrial discharge is set to 0.1 mg/L [15] [16].

Given the risks of contamination and the increased presence of chromium in aquatic and environmental ecosystems, a multitude of stringent analytical techniques for the removal of Cr (VI) were established. Thus, a wide range of techniques for the removal of Cr (VI) from aquatic environments is employed [17], including ion exchange methods [18], electrochemical processes [19], the use of bio-based materials [20], membrane filtration [21], adsorption [22], nanocomposites [23], etc. Recently, a variety of natural materials were used as adsorbents for the removal of Cr (VI) from aqueous solutions such as Ocimum americium kernels [24], Macadamia nuts [25], pistachio shells [26], etc. Yogeshwaran and Priya [27] reviewed several works on the removal of Cr (VI) from various natural adsorbents. Rai *et al.* [28] were the first who used mango kernel for Cr (VI) removal. In their study, they used activated carbon prepared from mango kernel powder activated with 40% H_3PO_4 and carbonized at 600˚C for 1 hour in an inert atmosphere.

However, in our study, mango kernel powder (MKP) was used directly as a bioadsorbent to removal Cr (VI) from aqueous media at the optimum pH. The

use of MKP is intended to offer an alternative that is less costly and less energetic than other conventional adsorbent materials such as activated carbon and sludge. In addition, mango is abundantly present in nature, and its application in the elimination of chromium does not require tedious treatment. Uv-visible spectrophotometry allowed to follow the absorbance of Cr (VI) then to quantify and evaluate its removal rate using Beer-Lambert law. The influence of pH, adsorbent mass, initial concentration of chromium, contact time, some thermodynamic parameters and kinetic evolution of Cr (VI) removal were also studied.

2. Materials and Methods

2.1. Chemical

To carry out this study, we used potassium dichromate ($K_2Cr_2O_7$, 99.7% m/m) as precursor for chromium ions, concentrated sulfuric acid (H_2SO_4, 98% m/v) and sodium hydroxide (NaOH, 98.8% m/m) were used to adjust the pH of the medium. These chemicals were purchased from Sigma Aldrich and used as received. Distilled water was used for the preparation of solutions. The bioadsorbent used in this study was mango kernel collected in Thies area (Senegal) and reduced to powder using an artisan mill.

2.2. Apparatus

In this study, we used beakers, a 250 mL volumetric flask and a stirrer coupled to a hot plate. Analysis was performed using a UV-visible absorption spectrophotometer (Thermo Scientific GENESYS 10S series, France) for absorbance measurements and for quantification. Adsorbent characterization was monitored using a Fourier transform infrared spectrophotometer (FTIR) (PerkinElmer, France), 8.300 - 350 cm^{-1}, resolution 0.4 cm^{-1}) to follow the evolution of absorption bands and occupied sites, energy dispersive X-ray spectroscopy (EDS) and scanning electron microscopes (SEM) (from Bruker Nano GmbH Berlin, Germany) to study surface morphology before and after contact between Cr (VI) and MKP.

2.3. Analytical Procedures

2.3.1. Adsorbate Preparation

Synthetic solution (100 mg/L) of potassium dichromate was prepared by dissolving a 25 mg mass in 250 mL of distilled water stabilized in optimal pH to promote the formation of Cr (VI). Working solutions were prepared in the range 10 - 100 mg/L by dilution and their absorbance was measured by UV-visible spectrophotometry at a wavelength of 350 nm, corresponding to the most resolved absorption band.

2.3.2. Optimization of Analytical Procedure

Some analytical parameters such as adsorbent mass, pH and contact time were optimized. Different masses of MKP (20 mg to 50 mg) were used to determine the optimal mass of adsorbent and the pH was varied from 1 to 10. The contact

time between adsorbent and chromium was varied in 5-minute intervals, from 5 to 30 minutes. Finally, the effect of the initial chromium concentration ranging from 10 - 100 mg/L was studied under an optimal pH that favors Cr (VI) formation. After stirring, the solutions were left to rest before being filtered and their absorbance were measured. Also, calculations were done for the determination of the percentage removal of Cr (VI) ions (%R), the adsorption capacities at time t (q_t, mg/g) and at equilibrium (q_e, mg/g) using the Equations (1)-(3) [29] [30].

$$\%R = \frac{C_0 - C_t}{C_0} \times 100 \tag{1}$$

$$q_e = \frac{C_0 - C_e}{m} \times V \tag{2}$$

$$q_t = \frac{C_0 - C_t}{m} \times V \tag{3}$$

where C_0 is the initial chromium concentration (mg/L); C_t the chromium concentration at time t (mg/L); C_e the chromium concentration at equilibrium (mg/L); V is the volume of the bulk solution (L) and m the mass of the adsorbent (g).

2.3.3. Study of Kinetic Parameters

After determining the optimal experimental conditions such as the initial concentration of Cr (VI) ions in the solution, the adsorbent mass, pH and stirring time, we studied the kinetic parameters. The use of first-order and second-order kinetic models [21] [31] represented by Equations (4) and (5), respectively, allowed us to plot time t as a function of $\log(q_e - q_t)$ and time as a function of t/q_t.

$$\ln\left(q_e - q_t\right) = \ln\left(q_e\right) - k_1 t \tag{4}$$

$$\frac{1}{q_t} = \frac{1}{k_2 q_e^2} + \frac{t}{q_e} \tag{5}$$

where q_e and q_t (mg/g) are the quantities of Cr (VI) adsorbed at equilibrium and at time t (h), respectively, and k_1 (h^{-1}) and k_2 (g/mg/h) are the first and second order kinetic rate constants.

2.3.4. Study of Isothermal Adsorption

The ionic distribution on the surface of the adsorbent at equilibrium for a given temperature is materialized by the study of the adsorption isotherm using empirical formulas. The linear isotherm models of Langmuir, Freundlich and Temkin [16] [32] [33] were used in the study and are represented by the following equations:

$$\text{Langmuir:} \quad \frac{C_e}{q_e} = \frac{1}{q_m k_L} + \frac{C_e}{q_m} \tag{6}$$

$$\text{Freundlich:} \quad \log q_e = \log k_f + \frac{1}{n} \log C_e \tag{7}$$

$$\text{Temkin:} \quad q_e = \frac{RT}{b_t} \ln\left(a_t C_e\right) \tag{8}$$

where q_e (mg/g) and C_e (mg/L) represent the adsorption capacity and aqueous phase concentration of the adsorbate at equilibrium respectively; q_m (mg/g) and k_L (L/mg) correspond to the monolayer capacity and Langmuir equilibrium related to the free energy of adsorption; the constants k_f (L/mg) and $1/n$ represent the capacity and intensity of Freundlich adsorption; a_t (L/g) and b_t (kJ/mol) are Temkin's isothermal constants; R is the universal gas constant (8.314 J/K/mol) and T is the temperature in Kelvin.

2.3.5. Study of Thermodynamic Parameters

The study of these parameters was carried out in a temperature range of 298 to 328 K and the thermodynamic variables such as the Gibbs free energy are given by the following relations:

$$k_c = \frac{C_{ad}}{C_e} \tag{9}$$

$$\Delta G° = -RT \ln k_c \tag{10}$$

$$\ln k_c = \frac{\Delta S°}{R} - \frac{\Delta H°}{RT} \tag{11}$$

where k_c is the equilibrium adsorption constant, C_e and C_{ad} (mg/L) represent the equilibrium and Cr (VI) concentrations adsorbed by the adsorbent respectively, R is the universal gas constant (8.3145 J/mol/K) and T is the temperature in Kelvin.

3. Results and Discussions

3.1. Influence of Some Parameters on Cr (VI)

3.1.1. Effect of Initial Chromium Concentration and Absorbent Dose

When the initial chromium concentration varied between 10 - 100 mg/L and MKP fixed at 45 mg under 25 min contact time, we noted that an increasing in adsorption capacity from 0.55 mg/g to a limit corresponding to the maximum adsorption capacity (22.51 mg/g), which could correspond to a saturation of all available fixation sites (**Figure 1(a)**). In addition, the percentage of chromium removal decreased from 94.87% to 45% as the initial chromium concentration increased (**Figure 1(a)**). These results give information on the concentration at which all sites are occupied and the excess amount of chromium remaining in the solution. The maximum adsorption capacity was obtained with a initial chromium concentration of 80 mg/L, so this value was used as the optimal solute (adsorbent) concentration for the following studies. This concentration is well above OMVS standards. According to the World Health Organization (WHO), the maximum permissible level of Cr (VI) in drinking water is 50 µg/L [15] [16] [34]. However, if we look at the variation in the mass of adsorbent, **Figure 1(b)** shows that the adsorption capacity decreases from 151 to 8 mg/g while, at the same time, the percentage of chromium ion removal increases from 93% to 97.4%.

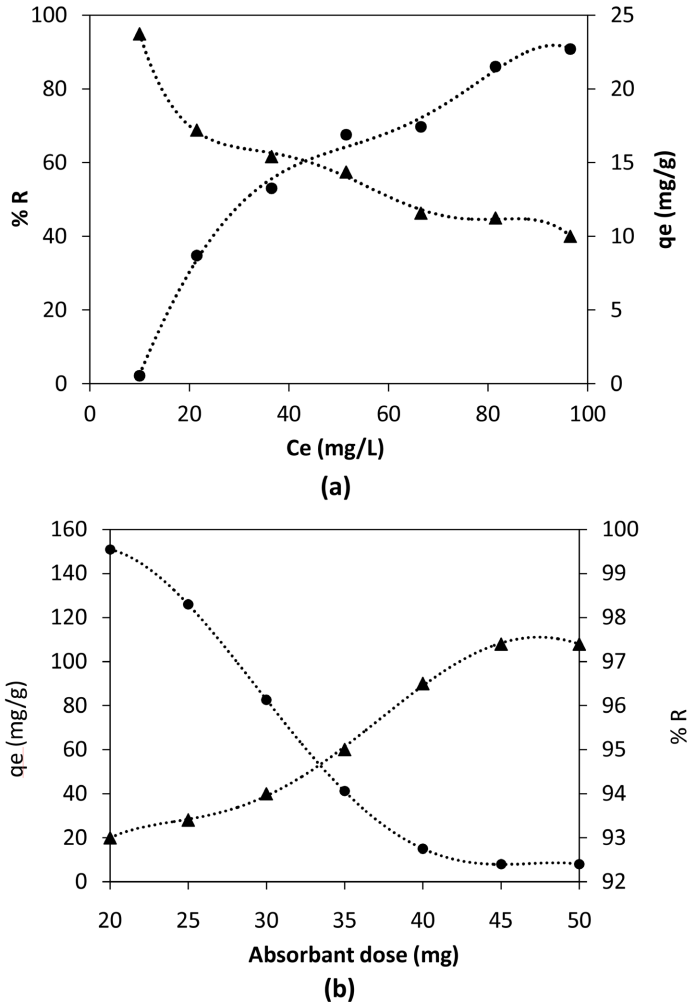

Figure 1. (▲) Evolution of percentage of chromium removal (R) and (●) adsorption capacity (q_e) *vs.* chromium initial concentration (a), *vs.* mass MKP (b).

These results can be explained by the fact that with a small amount of adsorbent, all the active sites are completely occupied by Cr (VI) ions. The excess of chromium in solution leads to a surface saturation of the adsorbent, resulting in a maximum adsorption capacity. However, only the increase of the adsorbent mass can cause an elimination of the excess of Cr (VI) ions in the solution by the creation of new fixation sites, hence a decrease of the adsorption capacity. On the other hand, the increase in the percentage of removal as a function of the adsorbent mass could be explained by the high recovery power (higher adsorption capacity) of MKP. As the concentration of chromium in the solution remains constant, there will be more binding sites resulting in an increase in the amount of at a constant temperature, there will be more binding sites resulting in an increase in the quantity of Cr (VI) ions collected by the adsorbent, thus increasing the percentage of removal [35]. Thus an optimal mass of 45 mg was found to remove up to 97% of Cr (VI) ions contained in the optimal concentration solution (**Figure 1(b)**).

3.1.2. Effect of pH and Contact Time

The pH of the solution and contact time are important parameters in determination of the types of chromium formed and adsorption capacity efficiency (Figure 2). Acidic pH (pH = 2) as can be seen in Figure 2(a) was considered to be able to promote the formation of chromium (VI) [36]. Chromium (VI) is in the form of $HCrO_4^-$, $Cr_2O_7^{2-}$ or CrO_4^{2-}, depending on the pH value and the concentration of the solution [37]. The $HCrO_4^-$ and $Cr_2O_4^{2-}$ forms are mainly available at equilibrium for pH values $0 \le pH \le 6$ [26]. If the pH is above or equal to 7, $Cr_2O_4^{2-}$ would be the predominant form in solution. This can be explain through the different pKa values for the chromate acid-base couples which are [38].

$pKa_1 = 0.75$ for $H_2CrO_4 / HCrO_4^-$ and $pKa_2 = 6.4$ for $HCrO_4^- / CrO_4^{2-}$.

We have a slight increase in Cr (VI) removal rate from 97% to 99.8% for a variation of pH between 1 and 2 (Figure 2(a)). These results show that at low pH, the $HCrO_4^-$ form predominates in the solution, which increases the adsorption capacity. This is due to the protonation of the adsorbent surface which

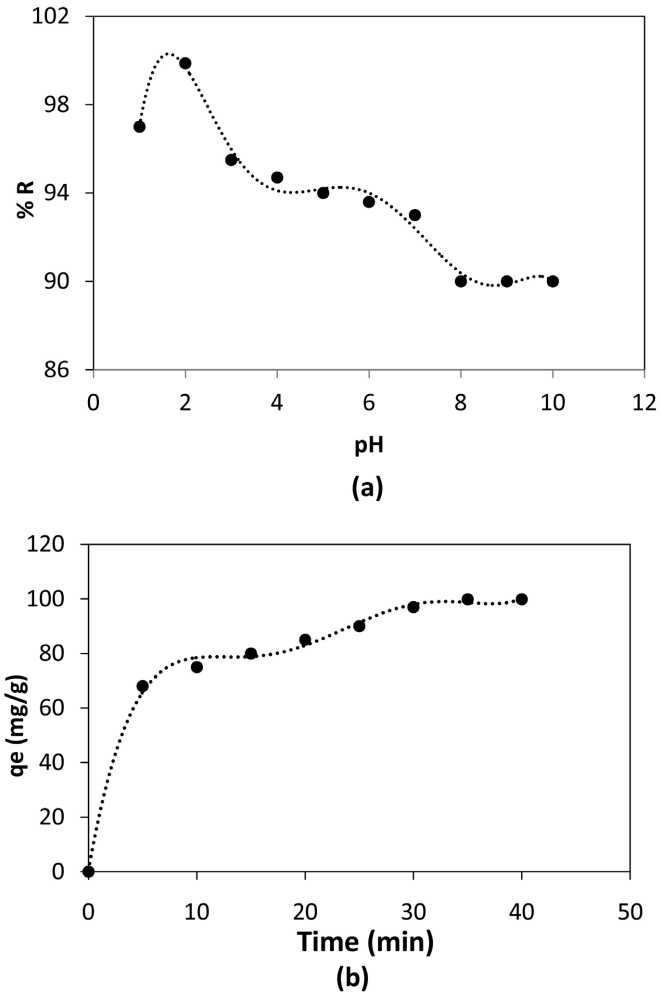

Figure 2. Evolution curves of percentage chromium removal *vs.* (a) pH and adsorption capacity vs. (b) contact time.

facilitates the electrostatic attraction between the chromium and the adsorbent [39]. On the other hand, there is a notable decrease in the rate of chromium removal until a constant value of 90% is reached at a pH of 8 (**Figure 2(a)**). This phenomenon can reflect the presence of negative charges on the surface of the adsorbent at a basic pH, which hinders the elimination of chromium. In a basic medium, the CrO_4^{2-} form is majority in solution because of the presence of OH^- resulting in electrostatic repulsion, thus causing competition between these negative ions [40].

Furthermore, **Figure 2(b)** shows that the percentage of chromium removal increases with contact time, reaching a limit value after 30 minutes. The availability of many active sites and a considerable concentration of chromium in the solution are the reasons for this increasing rate of chromium removal. After 30 min of contact between chromium and the adsorbent, the adsorption rate became constant due to the condensation of the active sites [41]. Consequently, the optimal equilibrium time for chromium adsorption by MKP under optimal pH conditions is 30 minutes.

3.1.3. Kinetic Study

Plots of $\log(q_e - q_t)$ and of t/q *vs.* time are shown in **Figure 3(a)** and **Figure 3(b)**, and all parameters are given in **Table 1**. The calculated q_e value (7.505 mg/g)

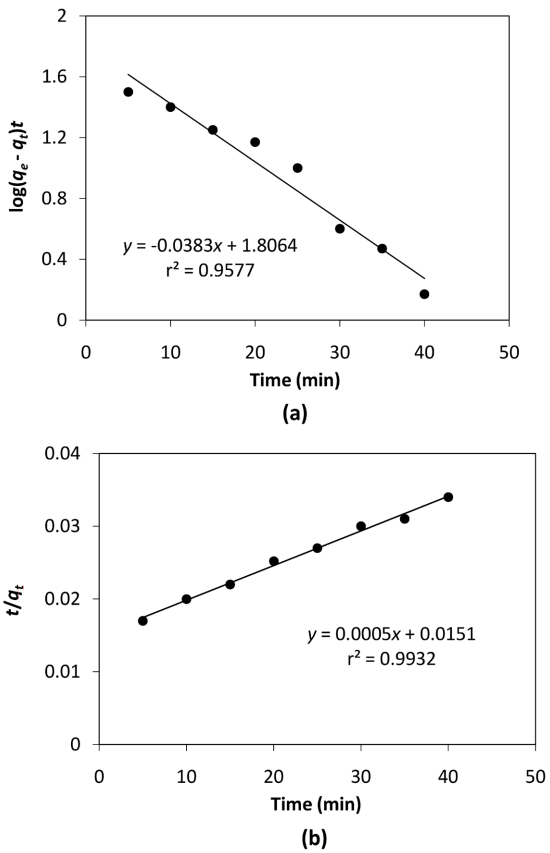

Figure 3. Curves for the pseudo-first order kinetics (a) and pseudo-second order kinetics (b).

Table 1. Kinetic parameters of chromium adsorption by MKP.

Kinetic model	Pseudo-first order				Pseudo-second order		
Parameters	q_{exp} (mg/g)	q_e (mg/g)	K_1 (h^{-1})	r^2	q_{exp} (mg/g)	K_2 (g/mg/h)	r^2
values	94.87	7.505	0. 938	0.958	100.00	0.027	0.993

is much lower than that experimentally obtained one (94.87 mg/g). This large discrepancy indicates the inadequacy of the pseudo-first order kinetic model. For the pseudo-second order kinetic model, the calculated q_e value (100.0 mg/g) is closer to the experimental value (94.87 mg/g). Thus, we can be concluded that the chromium adsorption process follows second order kinetics. The analysis of the table shows that the correlation coefficients (r^2) value obtained for the second order are closer to unity than for that first order. These results obtained with the second-order kinetics model, show that the concentrations of adsorbent and adsorbate are involved in the rate of removal, in the rate limitation, in the diffusion of particles and in the physico-chemical interaction between adsorbates and adsorbents in aqueous medium [42].

3.1.4. Isothermal Adsorption

The adsorption isotherm of Cr (VI) ions on MKP at different temperatures was studied (**Figure 4**) to understand the variation of adsorption as a function of adsorbate concentrations in solution [43]. Indeed, for the Langmuir model, the adsorbent surface must be absolutely homogeneous, *i.e.* in a monolayer form with a fixed number of adsorption sites, where adjacent adsorbates do not enter the process [44]. In contrast, the Freundlich model obeys a heterogeneity of the adsorbent surface favoring a multilayer formation due to the presence of adsorption sites with varying energies [45]. For Temkin's model, a decrease in adsorption heat is linear and not logarithmic and adsorption is characterized by a uniform distribution of binding energy up to a certain maximum point [46]. The results are reported in **Table 2**.

The adsorption constants of these models were evaluated and reported in **Table 2** with the corresponding correlation coefficients. The analysis of the results shows that the adsorption of chromium (VI) on MKP occurs according to the Freundlich model, which is in better agreement with the experimental data in terms of correlation coefficient (r^2 = 0.996), involves multilayer adsorption of Cr ions and occurs at inhomogeneous sites [47]. These results indicate that the system efficiently adapts through the heterogeneous Freundlich isotherm. Furthermore, the parameter value for the slope of the Freundlich curve of less than 1 indicates that the MKP has a heterogeneous surface structure. Similarly, the obtained n-value (n = 1.3) for the adsorption of Cr (VI) confirms that the adsorption is favorable [48]. Using the same Freundlich model, Fall *et al.* [23] obtained an adsorption capacity of 91.7 mg/g of Cr (VI) by the rGO@CNT@Fe_2O_3 nanocomposite for a contact time of 240 min at 298 K.

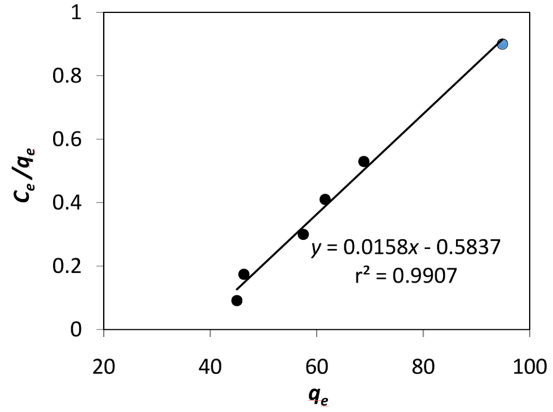

(a)

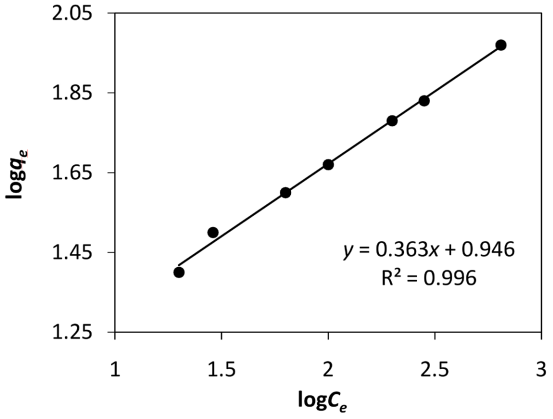

(b)

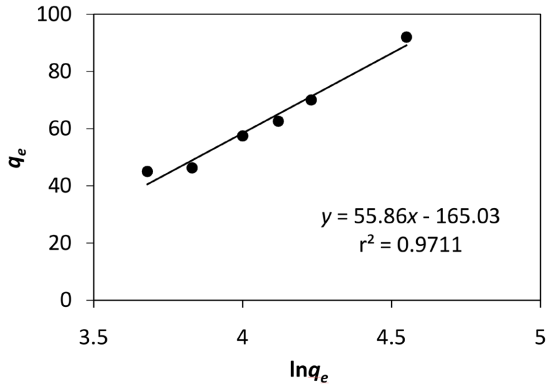

(c)

Figure 4. Langmuir isotherm (a), Friendly isotherm (b) and Temkin isotherm (c).

Table 2. Parameters of the isothermal models of Langmuir, Freundlich and Temkin for the removal of chromium by MKP.

Langmuir			Freundlich			Temkin		
q_m (mg/g)	K_L (L/mg)	r^2	K_f (L/mg)	$1/n$	r^2	a_t (L/g)	b_t (kJ/mol)	r^2
151	0.098	0.991	11.48	1.71	0.996	0.898	80.27	0.971

3.1.5. Thermodynamic Study

To study the thermodynamic parameters, we represented $\ln(k_c)$ as a function of the equilibrium concentration (Figure 5), the slope and intercept were used to determine the values of ΔH° and ΔS°. The results are shown in Table 3. If the temperature varies from 298 to 328 K, an increase in the quantity of adsorbed chromium is noted. From 328 K onwards, a plateau in chromium adsorption is observed, corresponding to the limit temperature. The negative values of ΔG° demonstrate that the adsorption process of Cr (VI) is spontaneous and feasible, and that the adsorption capacity of mango is high [49]. Furthermore, the positive and high value of ΔH° could be due to the MKP's strong attractive force and an increase in adsorption capacity [36].

The Cr (VI) adsorption process is spontaneous in the temperature range studied. It is therefore necessary to provide more information on the effect of temperature on the absorption process. For this, we calculated the inversion temperature (T_v) from the equation $\Delta G^\circ = 20.287 - 0.076T$ to know the direction of evolution of the system which is irreversible. As in equilibrium the process no longer evolves, $\Delta G^\circ = 0$ and $T_v = 267$ K. So for the process to be spontaneous ($\Delta G^\circ < 0$) the temperature must be higher than the inversion temperature ($T > T_v$). In conclusion, we can say that the thermodynamic study revealed that the Cr (VI) absorption process is thermodynamically favorable only at temperatures above 267 K.

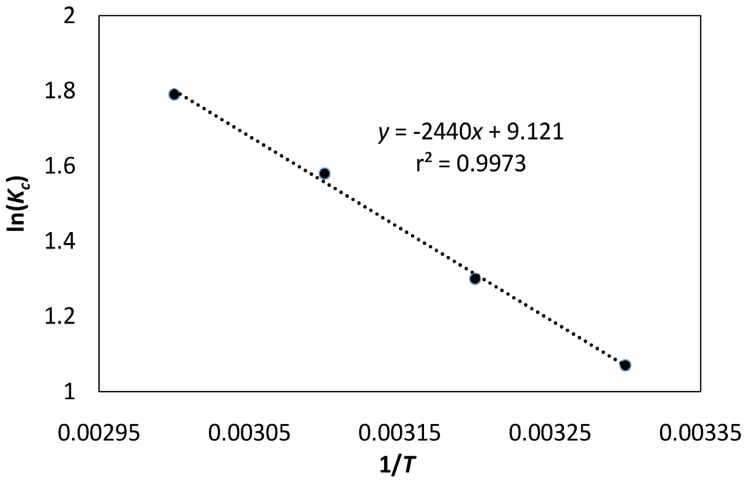

Figure 5. Thermodynamic study of the adsorption process (T = 328 K).

Table 3. Thermodynamic parameters of Cr (VI) adsorption by MKP.

Temperature (K)	ΔG° (kJ/mol)	ΔH° (kJ/mol)	ΔS° (kJ/K/mol)
298	−2.651	20.287	0.076
308	−3.149		
318	−4.441		
328	−4.881		

3.2. UV-Visible Spectroscopy Study of Cr (VI) Removal

Under optimum conditions, Uv-visible absorption is used to monitor Cr (VI) removal. The wavelength of maximum Cr (VI) absorption is recorded after a scan between 200 and 1000 nm. As can be seen in **Figure 6**, Cr (VI) presents three absorption bands at 210, 260 and 350 nm. The two energetic bands at 210 and 260 nm are less well resolved and disappear more quickly than the large band at 350 nm. These different peaks are thought to be due to electron transfer from the filled 2p orbitals of O^{2-} to the vacant 3d orbitals of the Cr (VI) ion. Sanchez-Hachair and Hofmann [39] attributed the last band at 350 nm to the chromium form $HCrO_4^-$ at pH 5. Some authors have reported that at an acidic pH (pH 2), the dominant form of Cr (VI) is $HCrO_4^-$, and that at higher pH, the other forms such as CrO_4^{2-} or $Cr_2O_7^{2-}$ are favored [28]. In another study, Subramaniam and Selvi [50] found the same three absorption bands that they attributed to Cr (VI) alone.

Also, we noted that the decrease of the absorbance bands (**Figure 6(a)**) is accompanied by the progressive discoloration of the solution (Graphical abstract) shows that Cr (VI) can be totally removed in all its forms by our adsorption device based on MKP after contact time of 30 min. Indeed, the oxygen atom in $Cr_2O_7^{2-}$ that acts as a ligand and due to charge transfer its one electron to chromium and due to which the colored compound is formed However, to ensure that the peaks obtained in absorption are due to Cr (VI) in its various forms and not to its reduction to Cr (III), we used cyclic voltammetry to check the electron exchange between Cr (VI) and the working electrode. The single reduction peak obtained (**Figure 6(b)**) shows that there is no reversible redox reaction between mango kernel powder and Cr (VI), and that Cr (VI) elimination occurs by trapping and adsorption (physisorption). Thus, the three absorption bands can be explained by the different forms of Cr (VI) in solution, such as $HCrO_4^-$, CrO_4^{2-} and $Cr_2O_7^{2-}$.

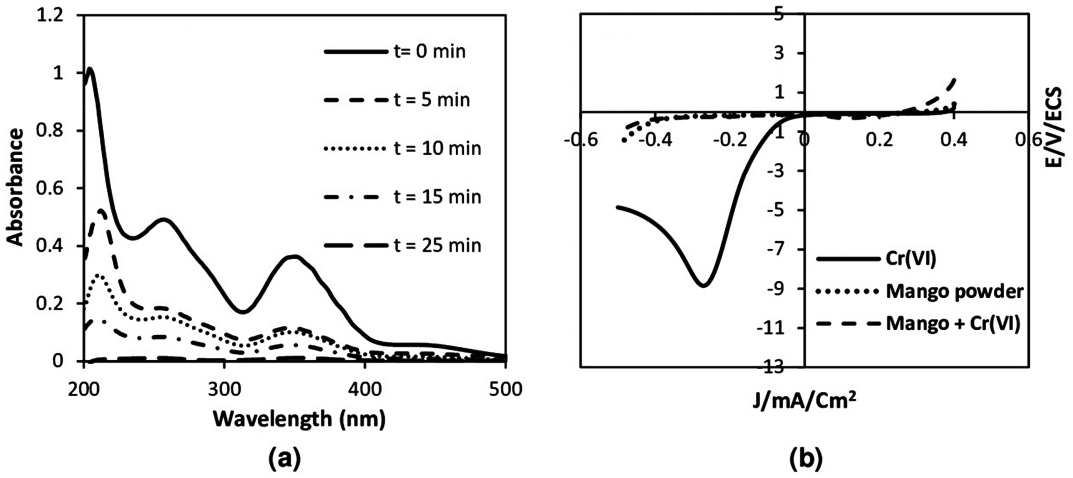

Figure 6. Adsorption spectra of 0.80 mg/L of Cr (VI) at different contact times with MKP (a) and Voltamograms of oxidation and reduction of Cr (VI) before and after treament (b).

3.3. Characterization of Adsorbent

3.3.1. FTIR Spectroscopy Analysis

We recorded infrared spectra before and after treatment to understand the retention mechanism of Cr (VI) ion by MKP (**Figure 7**). The absorption peaks localized at about 3306 cm^{-1} indicate the presence of free and intermolecular bonded hydroxyl groups [51]. Those around 2850 - 2921 cm^{-1} can be due to the presence of aldehydes, carbonyls, carboxylic acids and esters on the surface and N-H amine or amide at the waver number of 1619 cm^{-1} [51] [52]. The peak at 1453 cm^{-1} indicates the presence of aromatic groups, amines and hydrocarbons on the MKP surface [53]. Comparison of **Figure 7(a)** and **Figure 7(b)** reveals

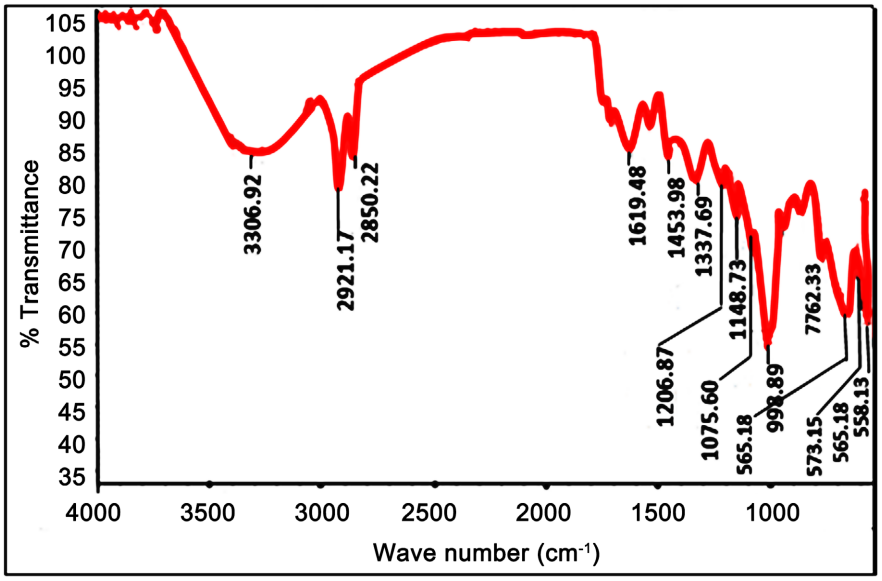

(a)

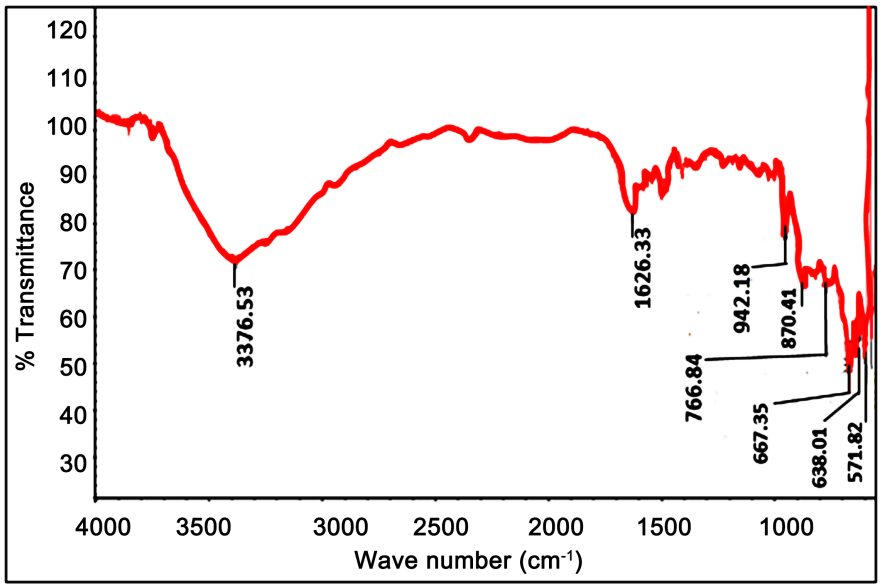

(b)

Figure 7. FTIR spectrum of MKP before (a) and after (b) adsorption of Cr (VI) ions.

the disappearance of several bands (at 2921, 2850, 1453, 1337, 1206, 1148, 1075, 998, 578, 573, 565, 558 cm^{-1}) corresponding to a total modification of the fingerprint of MKP and indicating the high affinity between Cr (VI) and its functional groups. The Cr (VI) elimination mechanism leads to the appearance of new peaks at 3376 and 1626 cm^{-1} due to stretching or deformation of the amine/amide N-H bond. Peaks appearing at 942, 870 and 766 cm^{-1} can be attributed to deformation of the C-H group of disubstituted aromatics. We can also confirm that these surface functional groups present in the adsorbent are involved in the main absorption processes by electrostatic interaction between the positively charged surface in acid medium due to the presence of H^+ ions in aqueous solution and the anionic Cr (VI) species ($HCrO_4^-$, CrO_4^{2-}, $Cr_2O_7^{2-}$) [54]. These multiple surface functional groups offer several binding sites for Cr (VI) and are responsible for MKP's high adsorption capacity.

3.3.2. SEM and EDS Characterization

The surface properties of MKP before and after contact with Cr (VI) was investigated (**Figure 8**). Comparison of **Figure 8(a)** and **Figure 8(b)** reveals a change in the morphology of the KMP, testifying to the adhesion of Cr (VI) to the adsorbent surface thanks to Van der Waals attraction. The EDS spectra, before (**Figure 8(c)**) and after (**Figure 8(d)**), show the retention of Cr (VI) by the adsorbent, which explains the change in morphology of the MKP surface. Another advantage of using MKP is its ability to retain sulfur from the sulfuric acid used

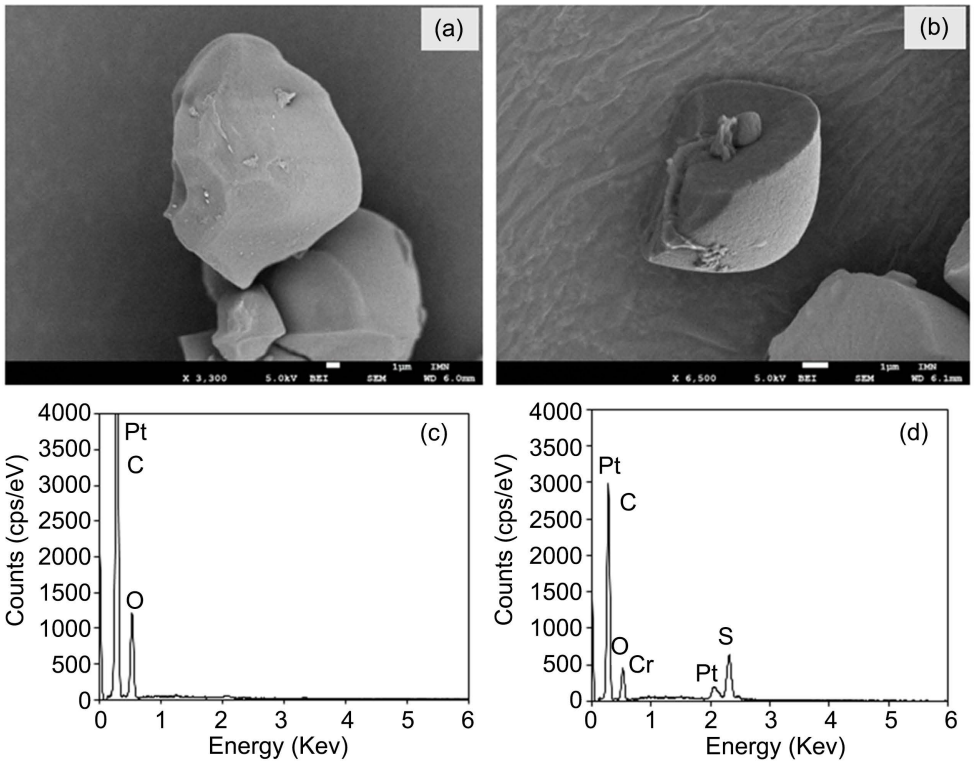

Figure 8. (a) and (b): SEM micrographs, (c) and (d): Energy-dispersive X-ray spectroscopy (EDS) spectra of MKP before and after adsorption of Cr (VI) (0.8 mg/L).

to adjust pH. In contrast to the mango kernel activated carbon used by Rai *et al.* [28], which has a highly porous structure with greater homogeneity and an average pore diameter of 38.9 μm allowing easy site occupation and almost similar FTIR spectra observed before and after Cr (VI) adsorption. However, in our study, **Figure 7** showed a profound change in the FTIR spectra before and after treatment, with changing and disappearing of several bands. Using SEM-EDS, other authors [28] [55] [56] have reported the change in adsorbent surface morphology that confirms the efficient removal of Cr (VI) by adsorption.

4. Conclusion

In this study, we demonstrated the ability of mango kernel powder (MKP) to eliminate chromium VI ions. So, we first optimized some parameters affecting chromium adsorption such as the initial concentration, the mass of the adsorbent, the pH of the solution, the contact time, the kinetics and the thermodynamics to enhance its elimination. The adsorption process of Cr (VI) on the adsorbent (mango powder) is endothermic in nature at high temperature. The positive value of ΔS° indicates the good affinity of the mango shell powder towards Cr (VI) ions and also shows that the disorder is high at the adsorbent/adsorbate interface during the binding of Cr (VI) ions on the active sites. The negative value of ΔG° shows that the adsorption process of Cr (VI) on our sorbent is thermodynamically favorable to $T > 267$ K. All this makes MKP a very efficient bioadsorbent material, from the point of view of contact time (adsorbent/absorbent) and percentage removal of Cr (VI) ions. Compared to other sorbents, whether bioadsorbents or synthesized sorbents, the results obtained with MKP in record time appear new and promising for researches devoted to heavy metal removal.

Conflicts of Interest

The authors declare no conflicts of interest regarding the publication of this paper.

References

[1] Adechina, R.A.M.A., Kelome, N.C., Kaki, C., Hounkpe, J.B. and Randriana, N.R.F. (2019) Evaluation of Contamination Risks in Metallic Trace Elements (MTE) in the Sediments of Ouémé Delta in Benin. *International Journal of Innovation and Applied Studies*, **27**, 943-954. http://www.ijias.issr-journals.org/

[2] Tiwari, A.K.I., Sunder, L.P., Srivastava, N., Shah, M., Ahmad, I., Alshahrani, M.Y. and Pal, D.B. (2022) Bioadsorbent and Adsorbent-Based Heavy Metal Removal Technologies from Waste Water: New Insight. *Biomass Conversion and Biorefinery*, **13**, 13335-13356. https://doi.org/10.1007/s13399-022-02343-1

[3] Campillo-Cora, C., Rodríguez-González, L., Arias-Estévez, M., Fernández-Calviño, D. and Soto-Gómez, D. (2021) Infuence of Physicochemical Properties and Parent Material on Chromium Fractionation in Soils. *Processes*, **9**, Article 1073. https://doi.org/10.3390/pr9061073

[4] Liu, Y., Ding, J., Lu, X. and You, H. (2018) Study on the DNA-Protein Crosslinks Induced by Chromium (VI) in SPC-A1. *IOP Conference Series: Earth and Envi-*

ronmental Science, **108**, Artilce ID: 042096.
https://iopscience.iop.org/journal/1755-1315
https://doi.org/10.1088/1755-1315/108/4/042096

[5] Ai, T., Jiang, X. and Lui, Q. (2018) Chromium Removal from Industrial Wastewater Using *Phyllostachys pubescens* Biomass Loaded Cu-S Nanospheres. *Open Biochemistry Journal*, **16**, 842-852. https://doi.org/10.1515/chem-2018-0073

[6] Tumolo, M., Ancona, V., De Paola, D., Losacco, D., Campanale, C., Massarelli, C. and Uricchio, V.F. (2020) Chromium Pollution in European Water, Sources, Health Risk, and Remediation Strategies, An Overview. *International Journal Environmental Research of Public Health*, **17**, Article 5438.
https://doi.org/10.3390/ijerph17155438

[7] Ahmadi, A., Foroutan, R., Esmaeili, H. and Tamjidi, S. (2020) The Role of Bentonite Clay and Bentonite clay@$MnFe_2O_4$ Composite and Their Physico-Chemical Properties on the Removal of Cr(III) and Cr(VI) from Aqueous Media. *Environnement Science and Pollution Research*, **27**, 14044-14057.
https://doi.org/10.1007/s11356-020-07756-x

[8] Liu, W., Li, J., Zheng, J., Song, Y., Shi, Z., Lin, Z. and Chai, L. (2020) Different Pathways for Cr (III) Oxidation: Implications for Cr (VI) Reoccurrence in Reduced Chromite Ore Processing Residue. *Environmental Science & Technology*, **54**, 11971-11979. https://doi.org/10.1021/acs.est.0c01855

[9] Giuseppe, G., Graziantonio, A., Catalano, A., Carocci, A. and Sinicropi, M.S. (2021) The Double Face of Metals: The Intriguing Case of Chromium. *Applied Sciences*, **11**, Article 638. https://doi.org/10.3390/app11020638

[10] Vendruscolo, F., da Rocha Ferreira, G.L. and Filho, N.R.A. (2017) Biosorption of Hexavalent Chromium by Microorganisms. *International Biodeterioration et Biodegradation*, **119**, 87-95. https://doi.org/10.1016/j.ibiod.2016.10.008

[11] Zarczynska, K. and Krzebietke, S. (2020) The Effect of Chromium on Ruminant Health**.** *Journal of Elementology*, **25**, 1644-2296.
https://doi.org/10.5601/jelem.2020.25.1.1963

[12] Pooja, S., Surendra, P.S., Sheetal, K.P. and Yen, W.T. (2022) Health Hazards of Hexavalent Chromium (Cr (VI)) and Its Microbial Reduction. *Bioengineered*, **13**, 4923-4938. https://doi.org/10.1080/21655979.2022.2037273

[13] Vale, M.S., do Nascimento, R.F., Leitao, R.C. and Santaella, S.T. (2016) Cr and Zn Biosorption by *Aspergillus niger*. *Environmental Earth Sciences*, **75**, Article No. 462. https://doi.org/10.1007/s12665-016-5343-9

[14] Hu, H., Guo, H., Chen, Y. and Yan, S. (2022) Sediment Geochemistry and Its Influence on Chromium Enrichment in Porewater from a Deep Aquifer in the Baiyangdian Basin, China. *Journal of Soils and Sediments*, **22**, 2815-2826.
https://doi.org/10.1007/s11368-022-03259-z

[15] Das, B.K., Das, P.K., Das, B.P. and Dash, P. (2021) Green Technology to Limit the Effects of Hexavalent Chromium Contaminated Water Bodies on Public Health and Vegetation at Industrial Sites. *Journal of Applied Biology & Biotechnology*, **9**, 28-35.

[16] Vaiopoulou, E. and Gikas, P. (2020) Regulations for Chromium Emissions to the Aquatic Environment in Europe and Elsewhere. *Chomosphere*, **254**, Article ID: 126876. https://doi.org/10.1016/j.chemosphere.2020.126876

[17] Wang, Y., Huang, L., Wang, Z., Wang, L., Han, Y., Liu, X. and Ma. T. (2019) Application of Polypyrrole Fexible Electrode for Electrokinetic Remediation of Cr (VI)-Contaminated Soil in a Main-Auxiliary Electrode System. *Chemistry Energy Journal*, **373**, 131-139. https://doi.org/10.1016/j.cej.2019.05.016

[18] Li, L.L., Feng, X.Q., Han, R.P., Zang, S.Q. and Yang, G. (2017) Cr (VI) Removal via Anion Exchange on a Silver-Triazolate MOF. *Hazardous Materials Journal*, **9**, 622-628. https://doi.org/10.1016/j.jhazmat.2016.09.029

[19] Sall, M.L., Diaw, A.K.D., Gningue-Sall, D., Chevillot-Biraud, A., Oturan, N., Oturan, M.A. and Aaron, J.J. (2017) Removal of Cr (VI) from Aqueous Solution Using Electrosynthesized 4-Amino-3-Hydroxynaphthalene-1-Sulfonic Acid Doped Polypyrrole as Adsorbent. *Environment Science Pollution Research*, **24**, 21111-21127. https://doi.org/10.1007/s11356-017-9713-y

[20] Mondal, M.H., Malik, S., Garain, A., Mandal, S. and Saha, B. (2017) Extraction of Natural Surfactant Saponin from Soapnut (*Sapindus mukorossi*) and Its Utilisation in the Remediation of Hexavalent Chromium from Contaminated Water. *Tenside Surfactants Detergents*, **54**, 519-529. https://doi.org/10.3139/113.110523

[21] Njoya, O., Zhao, S., Kong, X., Shen, J., Kang, J., Wang, B. and Chen, Z. (2021) Efficiency and Potential Mechanism of Complete Cr(VI) Removal in the Presence of Oxalate by Catalytic Reduction Coupled with Membrane Filtration. *Separation and Purification Technology*, **275**, Article ID: 118915. https://doi.org/10.1016/j.seppur.2021.118915

[22] Saravanan, A., Kumar, P.S., Govarthanan, M., George, C.S., Vaishnavi, S., Moulishwaran, B., Kumar, S.P., Jeevanantham, S. and Yaashikaa, P.R. (2021) Adsorption Characteristics of Magnetic Nanoparticles Coated Mixed Fungal Biomass for Toxic Cr (VI) Ions in Aquatic Environment. *Chemosphere*, **267**, Article ID: 129226. https://doi.org/10.1016/j.chemosphere.2020.129226

[23] Fall, B., Gaye, C., Niang, M., Yakubu, A.A., Diaw, A.K.D., Fall, M., Sabu, T. and Hyacinthe, R. (2022) Removal of Toxic Chromium Ions in Aqueous Medium Using a New Sorbent Based on rGO@CNT@Fe_2O_3. *Chemistry Africa*, **5**, 1809-1821. https://doi.org/10.1007/s42250-022-00499-x

[24] Vaddi, D.R., Gurugubelli, T.R., Koutavarapu, R., Lee, D.Y. and Shim, J. (2022) Bio-Stimulated Adsorption of Cr(VI) from Aqueous Solution by Groundnut Shell Activated Carbon@Al Embedded Material. *Catalysts*, **12**, Article 290. https://doi.org/10.3390/catal12030290

[25] Pakade, V.E., Ntuli, T. and Ofomaja, D.A.E. (2017) Ofomaja, Biosorption of Hexavalent Chromium from Aqueous Solutions by Macadamia Nutshell Powder. *Applied Water Science*, **7**, 3015-3030. https://doi.org/10.1007/s13201-016-0412-5

[26] Abdullahi, M.R. and Alkali, M.I. (2023) Removal of Chromium (VI) from Aqueous Solution Using Activated Carbon Derived from Modified Bambara Nut Shells (*Vignasubterranea* (L.) verdc.). *Journal of Applied Sciences and Environmental Management*, **27**, 421-431. https://www.ajol.info/index.php/jasem https://doi.org/10.4314/jasem.v27i3.4

[27] Priya, E. and Senthamil Selvan, P. (2017) Water Hyacinth (*Eichhornia crassipes*): An Efficient and Economic Adsorbent for Textile Effluent Treatment: A Review. *Arabian Journal of Chemistry*, **10**, S3548-S3558. https://doi.org/10.1016/j.arabjc.2014.03.002

[28] Rai, M.K., Shahi, G., Meena, V., Meena, R., Chakraborty, S., Singh, R.S. and Rai, B.N. (2016) Removal of Hexavalent Chromium Cr (VI) Using Activated Carbon Prepared from Mango Kernel Activated with H_3PO_4. *Resource-Efficient Technologies*, **2**, S63-S70. https://doi.org/10.1016/j.reffit.2016.11.011

[29] Frantz, T.S., Silveira, N., Quadro, M.S., Barcelos, A.A., Cadaval Jr., T.R.S. and Pinto, L.A.A. (2017) Cu(II) Adsorption from Copper Mine Water by Chitosan Films and the Matrix Effects. *Environment Science Pollution Research*, **24**, 5908-5917. https://doi.org/10.1007/s11356-016-8344-z

[30] Thue, P.S., Adebayo, M.A., Lima, E.C., Sieliechi, J.M., Machado, F.M., Dotto, G.L., Vaghetti, J.C.P. and Dias, S.L.P. (2016) Reparation, Characterization and Application of Microwave-Assisted Activated Carbons from Wood Chips for Removal of Phenol from Aqueous Solution. *Journal of Molecular Liquids*, **223**, 1067-1080. https://doi.org/10.1016/j.molliq.2016.09.032

[31] Kaur, J., Kaur, M., Ubhi, M.K., Kaur, N. and Greneche, J.M. (2021) Compposition Optimization of Activated Carbon-Iron Oxide Nanocomposite for Effective Removal of Cr (VI) Ions. *Materials Chemistry Physics*, **258**, Article ID: 124002. https://doi.org/10.1016/j.matchemphys.2020.124002

[32] Ai, T., Wu, S.Y., Zhang, R., Gao, M., Zhou, J., Xie, J., Li, R. and Zhang, Z. (2021) Changes in the Structure and Mechanical Properties of a Typical Coal Induced by Water Immersion. *International Journal of Rock Mechanics & Mining Sciences*, **138**, Article ID: 104597. https://doi.org/10.1016/j.ijrmms.2020.104597

[33] Araújo, C.S.T., Almeida, I.LS., Rezende, H.C., Marcionilio, S.M.L.O., Léon, J.J.L. and de Matos, T.N. (2018) Elucidation of Mechanism Involved in Adsorption of Pb(II) onto Lobeira Fruit (*Solanum lycocarpum*) Using Langmuir, Freundlich and Temkin Isotherms. *Journal Saoudien des Sciences Biologiques*, **137**, 348-354. https://doi.org/10.1016/j.microc.2017.11.009

[34] Sharifnia, S., Khadivi, M.A., Shojaeimehr, T. and Shavisi, Y. (2016) Characterization, Isotherm and Kinetic Studies for Ammonium Ion Adsorption by Light Expanded Clay Aggregate (LECA). *Journal of Saudi Chemical Society*, **20**, S342-S351. https://doi.org/10.1016/j.jscs.2012.12.003

[35] Ba, S., Alagui, A. and Hajjaji, M. (2018) Retention and Release of Hexavalent and Trivalent Chromium by Chitosan, Olive Stone Activated Carbon, and Their Blend. *Environmental Science and Pollution Research*, **25**, 19585-19604. https://doi.org/10.1007/s11356-018-2196-7

[36] Subedi, N., Lähde, A., Abu-Danso, E., Iqbal, J. and Bhatnagar, A. (2019) A Comparative Study of Magnetic Chitosan (Chi@Fe_3O_4 and Graphene Oxide Modified Magnetic Chitosan (Chi@Fe_3O_4/GO) Nanocomposites for Efficient Removal of Cr (VI) from Water. *International Journal of Biological and Macromolecules*, **137**, 948-959. https://doi.org/10.1016/j.ijbiomac.2019.06.151

[37] Xiang, L., Niu, C.G., Tang, N., Lv, X.X., Guo, H., Li, Z.W., Liu, H.Y., Lin, L.S., Yang, Y.Y. and Liang, C. (2021) Polypyrrole Coated Molybdenum Disulfde Composites as Adsorbent for Enhanced Removal of Cr (VI) in Aqueous Solutions by adsorptIon Combined with Reduction. *Chemical Engineering Journal*, **408**, Article ID: 127281. https://doi.org/10.1016/j.cej.2020.127281

[38] Shi, S., Yang, J., Liang, S., Li, M., Gan, Q., Xiao, K. and Hu, J. (2018) Enhanced Cr (VI) Removal from Acidic Solutions Using Biochar Modified by Fe_3O_4@SiO_2-NH_2 Particles. *Science Total Environment*, **628**, 499-508. https://doi.org/10.1016/j.scitotenv.2018.02.091

[39] Sanchez-Hachair, A. and Hofmann, A. (2018) Hexavalent Chromium Quantification in Solution: Comparing Direct UV-Visible Spectrometry with 1, 5-Diphenylcarbazide Colorimetdry. *Comptes Rendus Chimie*, **21**, 890-896. https://doi.org/10.1016/j.crci.2018.05.002

[40] Kumar, A. and Pandey, G. (2017) A Review on the Factors Affecting the Photocatalytic Degradation of Hazardous Materials. *Material Science & Engineering International Journal*, **1**, 106-114. https://doi.org/10.15406/mseij.2017.01.00018

[41] Homaidan, A.L., Qahtani, H.S., Al, A.A., Ghanayem, A.A., Ameen, F. and Ibraheem, I.B.M. (2018) Potential Use of Green Algae as a Biosorbent for Hexavalent Chromium Removal from Aqueous Solutions. *Saudi Journal of Biological Sciences*,

6, 1733-1738. https://doi.org/10.1016/j.sjbs.2018.07.011

[42] Guo, N., Lv, X., Li, Q., Ren, T., Song, H. and Yang, Q. (2020) Removal of Hexavalent Chromium from Aqueous Solution by Mesoporous *α*-FeOOH Nanoparticles: Performance and Mechanism. *Microporous and Mesoporous Materials*, **299**, Article ID: 110101. https://doi.org/10.1016/j.micromeso.2020.110101

[43] Chaithanya, T.K. and Yedla, S. (2010) Adsorption of Hexa-Valent Chromium Using Treated Wood Charcoal—Elucidation of Rate-Limiting Process. *Environmental technology*, **31**, 1495-1505. https://doi.org/10.1080/09593331003777144

[44] Czepirski, L., Balys, M.R. and Komorowska-Czepirska, E. (2000) Some Generalization of Langmuir Adsorption Isotherm. *Internet Journal of Chemistry*, **3**, 1099-8292.

[45] Da Silva Alves, D.C., Healy, B., Pinto, L.A.D.A., Cadaval Jr., T.R.S. and Breslin, C.B. (2021) Recent Developments in Chitosan-Based Adsorbents for the Removal of Pollutants from Aqueous Environments. *Molecules*, **26**, Article 594. https://doi.org/10.3390/molecules26030594

[46] Pandey, P.K., Sharma S.K. and Sambi, S.S. (2010) Kinetics and Equilibrium Study of Chromium Adsorption on zeoliteNaX. *International Journal of Environmental Science and Technology*, **7**, 395-404. https://doi.org/10.1007/BF03326149

[47] Sridevi, M., Nirmala, C., Jawahar, N., Arthi, G., Vallinayagam, S. and Sharma, V.K. (2021) Role of Nanomaterial's as Adsorbent for Heterogeneous Reaction in Waste Water Treatment. *Journal of Molecular Structure*, **1241**, Article ID: 130596. https://doi.org/10.1016/j.molstruc.2021.130596

[48] Vinhal, J.O., Nege, K.K., Lage, M.R., de M Carneiro, J.W., Lima, C.F. and Cassella, R.J. (2017) Adsorption of the Herbicides Diquat and Difenzoquat on Polyurethane Foam: Kinetic, Equilibrium and Computational Studies. *Ecotoxicology and Environment Safety*, **145**, 597-604. https://doi.org/10.1016/j.ecoenv.2017.08.005

[49] Pathania, D., Sharma, A. and Srivastava, A.K. (2020) Modelling Studies for Remediation of Cr (VI) from Wastewater by Activated *Mangifera indica* Bark. *Current Research in Green and Sustainable Chemistry*, **3**, Article ID: 100034. https://doi.org/10.1016/j.crgsc.2020.100034

[50] Subramaniam, P. and Selvi, P.T. (2013) Spectral Evidence for the One-Step Three-Electron Oxidation of Phenylsufinylacetic Acid and Oxalic Acid by Cr(VI). *American Journal of Analytical Chemistry*, **4**, 20-29. https://doi.org/10.4236/ajac.2013.410A1003

[51] Simha, P., Mathew, M. and Ganesapilla, M. (2016) Empirical Modeling of Drying Kinetics and Microwave Assisted Extraction of Bioactive Compounds from *Adathoda vasica* and *Cymbopogon citrates*. *Alexandria Engineering Journal*, **55**, 141-150. https://doi.org/10.1016/j.aej.2015.12.020

[52] Li, J., Lin, Q., Zhang, X. and Yan, Y. (2009) Kinetic Parameters and Mechanisms of the Batch Biosorption of Cr(VI) and Cr(III) onto *Leersia hexandra Swartz* Biomass. *Journal of Colloid Interface Science*, **333**, 71-77. https://doi.org/10.1016/j.jcis.2009.02.021

[53] OFomaja, A.E. and Naidoo, E.B. (2011) Biosorption of Copper from Aqueous Solution by Chemically Activated Pine Cone: A Kinetic Study. *Chemical Engineering Journal*, **175**, 260-270. https://doi.org/10.1016/j.cej.2011.09.103

[54] Karimi-Maleh, H., Ayati, A., Ghanbari, S., Orooji, Y., Tanhaei, B., Karimi, F., Alizadeh, M. Rouhi, J., Fu, L. and Sillanpää, M. (2021) Recent Advances in Removal Techniques of Cr (VI) Toxic Ion from Aqueous Solution: A Comprehensive Review. *Journal of molecular liquids*, **329**, Article ID: 115062. https://doi.org/10.1016/j.molliq.2020.115062

[55] Nasanjargal, S., Munkhpurev, B.A., Kano, N., Kim, H.J. and Ganchimeg, Y. (2021) The Removal of Chromium(VI) from Aqueous Solution by Amine-Functionalized Zeolite: Kinetics, Thermodynamics, and Equilibrium Study. *Journal of Environmental Protection*, **12**, 654-675. https://doi.org/10.4236/jep.2021.129040

[56] Zhang, L., Niu, W., Sun, J. and Zhou, Q. (2020) Efficient Removal of Cr(VI) from Water by the Uniform Fiber Ball Loaded with Polypyrrole: Static Adsorption, Dynamic Adsorption and Mechanism Studies. *Chemosphere*, **248**, Article ID: 126102. https://doi.org/10.1016/j.chemosphere.2020.126102